

# Journal of Materials Chemistry C

Accepted Manuscript



This is an *Accepted Manuscript*, which has been through the Royal Society of Chemistry peer review process and has been accepted for publication.

*Accepted Manuscripts* are published online shortly after acceptance, before technical editing, formatting and proof reading. Using this free service, authors can make their results available to the community, in citable form, before we publish the edited article. We will replace this *Accepted Manuscript* with the edited and formatted *Advance Article* as soon as it is available.

You can find more information about *Accepted Manuscripts* in the [Information for Authors](#).

Please note that technical editing may introduce minor changes to the text and/or graphics, which may alter content. The journal's standard [Terms & Conditions](#) and the [Ethical guidelines](#) still apply. In no event shall the Royal Society of Chemistry be held responsible for any errors or omissions in this *Accepted Manuscript* or any consequences arising from the use of any information it contains.

## ARTICLE

# Control of Plasmonic Fluorescence Enhancement on Self-Assembled 2-D Colloidal Crystals

Cite this: DOI: 10.1039/x0xx00000x

Wei Hong,<sup>‡</sup> Yu Zhang,<sup>‡</sup> Lin Gan, Xudong Chen\* and Mingqiu Zhang\*Received 00th January 2012,  
Accepted 00th January 2012

DOI: 10.1039/x0xx00000x

www.rsc.org/

Ordered arrays of Ag-capped colloidal crystals were fabricated and modified with conjugated polymers for evaluating excitation and emission fluorescence enhancement due to localized surface plasmon resonance (LSPR). The maximum enhancement accrued on the maximum overlap between the excitation wavelength and LSPRs of the substrates. The observed fluorescence enhancement and life time measurement showed that the large enhancement came from a combination of greatly enhanced excitation and an increased radiative decay rate leading to an associated enhancement of the quantum efficiency. Such Ag nanostructured arrays fabricated by colloidal lithograph thus show great potential for biosensing and photovoltaic applications, and the excitation wavelength-LSPR based fluorescence enhancement would prove useful for understanding and optimizing metal-enhanced fluorescence.

## Introduction

Metal induced fluorescence enhancement (MIFE) has attracted widespread research interests because of its promising applications, such as biosensing,<sup>[1]</sup> optics devices<sup>[2]</sup> and fluorescence-based imaging.<sup>[3]</sup>

Previous investigations demonstrated that MIFE originated from interactions of excited fluorophores with surface plasmon resonances (SPR) on metal structures.<sup>[4]</sup> Such interactions can lead to desirable effects including increased quantum yields, fluorescence decay rate, photostability and energy transfer rate. On the other hand, the fluorescence quenching effect competes with all these positive effects. It was indicated that fluorophore quenched within 5 nm from the surface of metal nanoparticles and the fluorescence reached maximum at about 10 nm from the metal surface.<sup>[5]</sup> For larger metal-fluorophore separation over 10 nm, the enhancement effect progressively declines. Thus, MIFE can be tuned by controlling the metallic particle composition, shape, interparticle distance and fluorophore-metal distance.<sup>[6]</sup>

Plasmonic structures with precise geometry are mostly fabricated using nanoimprint lithography,<sup>[7]</sup> focused ion beam lithography and electron beam,<sup>[8]</sup> which have the disadvantages of high cost, complicated process and limited sample area. Other notable methods used for fluorescence enhancement on planar substrates include physical adsorption of Ag/Au colloids<sup>[9]</sup> and chemical deposition of Ag/Au films<sup>[10]</sup> on glass. However, the LSPR and the resulting plasmonic enhancements from these noble metal substrates could not be systematically turned.

Recently, nanosphere lithography (NSL) has been used to fabricate large area plasmonic nanostructure.<sup>[11]</sup> Their optical properties are usually explained by the coupling of localized surface plasmon resonances (LSPRs) with surface plasmon polaritons (SPPs) along the periodical metal-dielectric interface,

called as Bragg plamons.<sup>[12]</sup> Great success has been achieved in fluorescence enhancement<sup>[13]</sup> and surface-enhanced Raman scattering (SERS)<sup>[14]</sup> based on electromagnetic enhancement from the NSL structure.

However, most of fluorescence enhancements based on Ag/Au colloids, Ag/Au films and NSL array have been directed at fluorophores of small molecules whose excitation wavelength and emission wavelength were very close to each other, leading to simultaneous overlaps of LSPR with both excitation and emission wavelength.<sup>[8-10, 13]</sup> Thus, it was not clear whether the major contribution of LSPR was to increase the excitation or the emission. Such question would become more important if more complex plasmonic substrates are fabricated, where several physical mechanisms contribute to the observed fluorescence enhancements.

In addition, most of the reported fluorescence enhancements based on NSL structures focused on internal diameters within a short range around the wavelength of visible light.<sup>[13]</sup> Thus challenges remain to have a more comprehensive comparison between NSL structures from subwavelength to micrometer level, as well as disordered NSL structures.

In this work, we report a systematic study about the fluorescence enhancement influenced by the Ag-capped colloidal crystal whose sphere diameter ranges from 200 to 1000 nm. Conjugated polymers, whose excitation maxima and emission maxima are over 100 nm from each other, are taken as fluorophores, hence simultaneous overlaps between excitation/emission wavelength and LSPR could be prevented. Excitation enhancement and emission enhancement are semi-quantitatively separated by analyzing the fluorescence lifetime. Experimental and theoretical results show that the fluorescence enhancement observed is attributed to increased excitation rate from the overlap of excitation wavelength with LSPR of the Ag-capped colloidal crystal array and higher quantum yield from the increased intrinsic decay rate of the fluorophores.

## Experimental

### Reagents

Poly[5-methoxy-2-(3-sulfopropoxy)-1,4-phenylenevinylene] potassium salt solution (MPS-PPV, 0.25 wt. % in H<sub>2</sub>O), poly(3-hexylthiophene-2,5-diyl) (P3HT,  $M_n=1.5-4.5 \times 10^3$ ), 3,6-dibromo-9-octylcarbazole, 2,5-bis-(4-bromo-phenyl)-[1,3,4]-oxadiazole, 2,7-diethyne-9,9'-dioctyluorene and Pd(PPh<sub>3</sub>)<sub>2</sub>Cl<sub>2</sub> were purchased from Sigma-Aldrich. Other solvents and chemicals were purchased from local suppliers. All reagents were used without further purification unless specified otherwise.

### Preparation of two-dimensional polystyrene (PS) colloidal crystals

Monodispersed colloidal particles of PS (200–1000 nm diameter, approximately 3% standard deviation) were synthesized by precipitation-emulsion polymerization using 2,2-azobisisobutyronitrile (AIBN) as initiator and polyvinylpyrrolidone (PVP) as stabilizer,<sup>[15]</sup> or purchased commercially (Alfa Aesar Corporation/Invitrogen). Briefly, 25 ml styrene, 3 g PVP and 1 g AIBN were dispersed in 75 mL methanol, stirred intensively with a magnetic beater at 298 K. The reaction mixture was kept under UV-irradiation at room-temperature with continuous stirring. After 24 h, the colloidal particles were obtained by centrifugation and rinsed 3 times with anhydrous ethanol and 2 times with pure water to remove PVP. The size of the PS spheres could be controlled by the quantity of styrene. The obtained monodispersed PS particles were dispersed in anhydrous ethanol to give a weight concentration of 2.5 wt%.

A drop (ca. 15  $\mu$ L) of the PS suspension was pipetted onto the whole of a quartz slide (with a diameter of 2.5 cm, cleaned by a plasma cleaning system). PS colloidal monolayer was achieved by a floating operation after the suspension was completely dried,<sup>[16]</sup> and the monolayer was picked up with a quartz slide to form a two-dimensional polystyrene colloidal crystals.

### Synthesis of N-octylcarbazole-co-9,9'-dioctyluorene-co-1,3,4-oxadiazole copolymer (PCFOz)

Synthesis of light-emitting conjugated polymer PCFOz was carried out by an improved method based on previous literatures.<sup>[17]</sup>

Briefly, Sonogashira reaction of 3,6-dibromo-9-octylcarbazole, 2,5-bis-(4-bromo-phenyl)-[1,3,4]-oxadiazole and 2,7-diethyne-9,9'-dioctyluorene (molar ratio= 0.56 mmol : 0.97 mmol : 1.45 mmol) via Pd(PPh<sub>3</sub>)<sub>2</sub>Cl<sub>2</sub> and CuI catalyzing was carried out under refluxing condition, followed by trimethylamine treatment. The copolymer was purified by chromatography using silica support. <sup>1</sup>H NMR (300 MHz, CDCl<sub>3</sub>),  $\delta$  ppm (mult., integr.): 8.22–8.09 (t, 3H), 8.06–7.96 (d, 6H), 7.81–7.61 (t, 8H), 7.61–7.42 (m, 7H), 3.55 (s, 11H), 2.01 (s, 10H), 1.41–0.48 (m, 50H). GPC:  $M_n=1.5 \times 10^5$  g mol<sup>-1</sup>, PDI=1.36.

### Substrate fabrication

The quartz slides with 2-D polystyrene colloidal crystals were mounted into the chamber of a Quorum Q150TES automatic high vacuum coating system for Ag sputtering deposition with thickness of 2.5–40 nm.

After the Ag deposition, the substrates were coated with a polyvinyl acetate (PVA) spacer layer about 10 nm thick by spin-coating, followed by a second time spin-coating for the fluorophore

layers using 0.1 mg ml<sup>-1</sup> PCFOz toluene solution, 0.5 mg ml<sup>-1</sup> MPS-PPV 3:7 v/v ethanol/aqueous solution, 1 mg ml<sup>-1</sup> P3HT toluene solution and 1 mM rhodamine B, fluorescein sodium, acriflavine ethanol solutions.

### Characterization

<sup>1</sup>H NMR spectra were obtained by a Varian Mercury-Plus 300 NMR spectrometer. Number-average molecular weight ( $M_n$ ) and the molecular weight distribution (PDI) were determined by gel permeation chromatography analysis (GPC, Waters Breeze). Reflectance spectra and extinction spectra were collected by a Lambda 750 UV-vis-NIR spectrometer. The quantum yield of PCFOz was measured by Hamamatsu absolute PL quantum yield spectrometer C11347. The scanning electron microscopic (SEM) pictures were obtained using a Hitachi S-4800 SEM with an accelerating voltage of 10 kV. The samples were arc coated with a thin gold film in advance. The transmission electron microscopic (TEM) pictures and the energy dispersive spectrum analysis were obtained on JEOL JEM-2010H TEM with an accelerating voltage of 200 kV. X-ray Photo-electron Spectroscopy (XPS) was measured on ESCALAB 250 (ThermoFisher Scientific) equipped with a monochromatic X-ray source (Al K $\alpha$ , 1486.6 eV).

Photoluminescence spectra were measured with a FLS920-Combined Time Resolved & Steady State Fluorescence Spectrometer (Edinburgh Instruments) using the 400 nm line of an Xe lamp as the excitation source and R1527 photomultiplier tube as the detector. Fluorescence decay curves were measured using the time-correlated single photon counting technique and a LifeSpec II luminescence spectrometer (Edinburgh Instruments, Ltd). The wavelength, pulse width, and repetition rate were 405 nm, 100 ps and 5 MHz, respectively. The experimental fluorescence lifetime accuracy was 6 ps.

The fluorescence decay curves were fitted using a double exponential fitting model:

$$I(t)=a_1e^{-t/t_1}+a_2e^{-t/t_2} \quad (1)$$

where  $t_1$  and  $t_2$  are two decay times;  $a_1$  and  $a_2$  are their weighting fractions.

The fluorescence enhancement ratio ( $E_f$ ) of the Ag-capped 2-D colloidal crystals is defined as

$$E_f=E_{cc,Ag}/E_{quartz} \quad (2)$$

where  $E_{cc,Ag}$  is the fluorescence intensity of the conjugated polymer on Ag-capped colloidal crystals (or flat Ag films with the same thickness),  $E_{quartz}$  is the fluorescence intensity of the conjugated polymer on a quartz surface. The data were averaged over five samples for each case.

### Computational modelling

Finite difference time domain (FDTD) method was used for calculation of the optical and electromagnetic properties of the Ag-capped 2-D colloidal crystals. All FDTD calculations were carried out on OptiFDTD 10. The input wave was defined with Gaussian modulated continuous wave. The observation objects was placed parallel to the plane of the 2-D colloidal crystals through the sphere centers (see Fig.S1).

## Results and discussion

### 3.1 Ag-capped 2-D colloidal crystals and their plasmonic resonance

The SEM images in **Fig.1a-c** show the high ordering of the hexagonal Ag-capped 2-D colloidal crystals formed by self-assembly with a domain size about 10  $\mu\text{m}$ . **Fig.1d** further exhibits that the Ag-capped 2-D colloidal crystals brightly diffract the incident light back toward the observer, demonstrating high ordering of the hexagonal 2-D array of PS spheres.

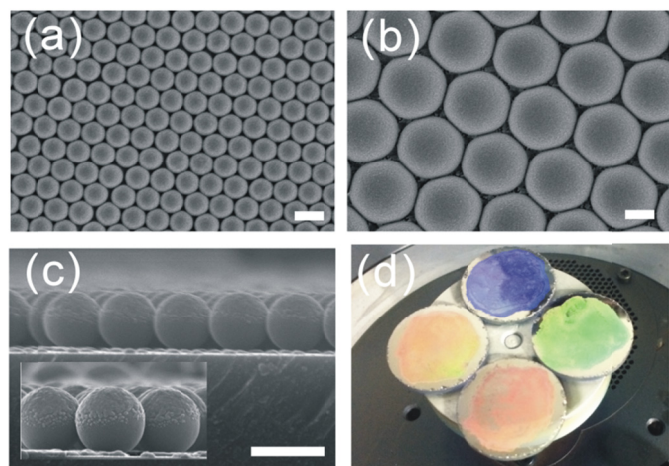


**Figure 1** SEM images of the 20-nm-Ag-capped 2-D colloidal crystals with diameter of (a) 400 nm and (b) 1000 nm. (c) Cross section of the Ag-capped 2-D colloidal crystals with diameter of 400 nm. Inset: enlarged image showing the Ag-capped sphere structure. (d) Photograph showing bright diffraction light from the 2-D colloidal crystals array after Ag deposition. Scale bar: 500 nm.

**Fig.2** shows the reflectance spectra for the hexagonal Ag-capped 2-D colloidal crystals with sphere diameter from 200 to 1000 nm (refer to PS200/Ag, PS300/Ag, PS400/Ag, PS600/Ag and PS1000/Ag, respectively). SEM images of the 2-D colloidal crystals capped by Ag with different thickness were given in **Fig.S2**, indicating that the Ag cap became continuous when the thickness exceeded 20 nm. Generally, increasing the Ag thickness could lead to greater fluorescence enhancements, but further increasing the Ag thickness over 20 nm can only enhance the fluorescence very slightly (see **Fig.S3**). Therefore, the thickness of Ag caps was fixed at 20 nm in this work. The plasmonic fluorescence enhancements on the Ag-capped 2-D colloidal crystals prepared by different deposition conditions were found to be very close to each other as long as the thicknesses of the silver films were the same (see **Fig.S4**). Elemental analysis measured by EDS and XPS indicated slight oxidation on the very surface of the silver films (see **Fig.S5**).

**Fig.3** shows the simulated electric field enhancement of PS300/Ag at the wavelengths of 410, 560 and 650 nm, respectively. Clearly, the field enhancement at 410 nm is greater than those at 560 and 650 nm. Further comparison between PS300/Ag, PS400/Ag and PS600/Ag were presented in **Fig.S6**. The simulation results supported that the increasing diameters of 2-D colloid crystals array, from 300 to 400 to 600 nm, resulted in the redshift of plasmonic peaks from 410 to 560 to 650 nm, respectively, corresponding to the reflectance spectra in **Fig.2**. After the PVA coating, the LSPR of the samples changed in width slightly without significant shift in maxima, as shown in the reflectance spectra and extinction spectra in **Fig.S8**, as well as the FDTD simulations in **Fig.S7**.

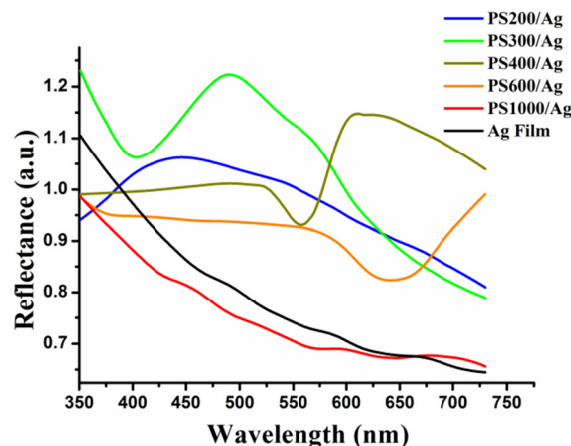


**Figure 2** Reflectance spectra of 20-nm-Ag-capped PS 2-D colloidal crystals with various sphere diameters (200-1000 nm) on quartz substrates.

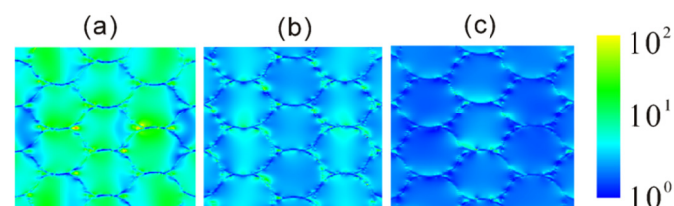


**Figure 3** Calculated relative electric field enhancement around the PS300/Ag in air at (a) 410 nm, (b) 560 nm and (c) 650 nm, respectively.

Disordered NSL samples were obtained over a wide range of volume compositions 200 nm : 300 nm : 400 nm =  $(1-x)/2$  :  $x$  :  $(1-x)/2$  (PS spheres for disordered PS300/Ag), and 200 nm : 400 nm : 600 nm =  $(1-x)/2$  :  $x$  :  $(1-x)/2$  (PS spheres for disordered PS400/Ag), where  $x$  could range from 0.4~0.9. **Fig.S9** showed the SEM images of the disordered NSL samples, indicating that the typical hexagonal structure of NSL disappeared when  $x$  went down to 0.7. In addition, the 2-D structure seemed to be stacked with the disorder degree rising. Extinction spectrum in **Fig.S10** indicated that the introduction of 60 vol% inhomogeneous microspheres led to significant decrease of LSPR.

### 3.2 Fluorescence enhancement of the Ag-capped 2-D colloidal crystals

Light-emitting conjugated polymers of PCFOz ( $\lambda_{\text{ex}}$ =405 nm,  $\lambda_{\text{em}}$ =515 nm), MPS-PPV ( $\lambda_{\text{ex}}$ =460 nm,  $\lambda_{\text{em}}$ =600 nm), P3HT ( $\lambda_{\text{ex}}$ =555 nm,  $\lambda_{\text{em}}$ =655 nm) and small fluorescent molecules of rhodamine B ( $\lambda_{\text{ex}}$ =565 nm,  $\lambda_{\text{em}}$ =610 nm), fluorescein sodium ( $\lambda_{\text{ex}}$ =507 nm,  $\lambda_{\text{em}}$ =550 nm), acriflavine ( $\lambda_{\text{ex}}$ =455 nm,  $\lambda_{\text{em}}$ =560 nm) were taken as examples to study the impacts of the Ag-capped 2-D colloidal crystals on the fluorescent layers.

**Fig.4-6** and **Fig.S11-13** showed the fluorescence measurements of the five fluorophores layer on quartz, flat Ag film and different Ag-capped 2-D colloidal crystals substrates. The highest fluorescence enhancement observed for PCFOz ( $\lambda_{\text{ex}}$ =405 nm, **Fig.4**), MPS-PPV ( $\lambda_{\text{ex}}$ =460 nm, **Fig.5**), and acriflavine ( $\lambda_{\text{ex}}$ =455 nm, **Fig.S11**) were from samples of PS300/Ag (LSPR at 410 nm), while the highest fluorescence enhancement observed for P3HT ( $\lambda_{\text{ex}}$ =555 nm, **Fig.6**),

rhodamine B ( $\lambda_{\text{ex}}=565$  nm, **Fig.S12**) and fluorescein sodium ( $\lambda_{\text{ex}}=507$  nm, **Fig.S13**) were from samples of PS400/Ag (LSPR at 560 nm).

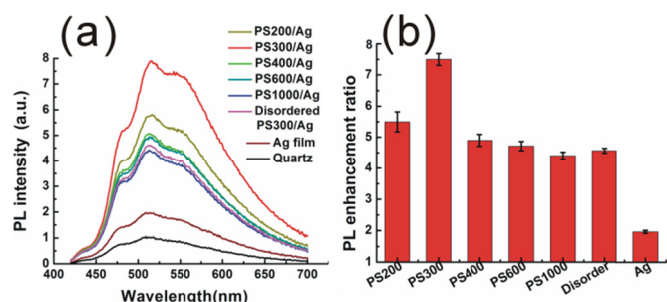


**Figure 4** (a) Fluorescence spectra of conjugated polymer PCFOz layer on different substrates ( $\lambda_{\text{ex}}=405$  nm). (b) Enhancement ratio of different substrates at  $\lambda_{\text{em}}=515$  nm.

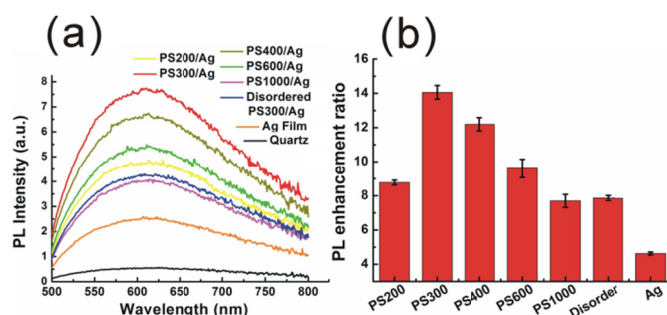


**Figure 5** (a) Fluorescence spectra of conjugated polymer MPS-PPV layer on different substrates ( $\lambda_{\text{ex}}=460$  nm). (b) Enhancement ratio of different substrates at  $\lambda_{\text{em}}=600$  nm.

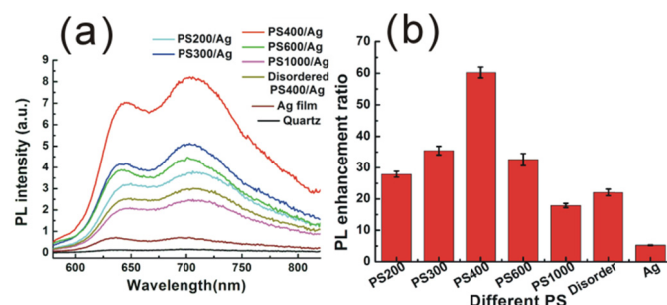


**Figure 6** (a) Fluorescence spectra of conjugated polymer P3HT layer on different substrates ( $\lambda_{\text{ex}}=555$  nm). (b) Enhancement ratio of different substrates at  $\lambda_{\text{em}}=655$  nm.

The change of fluorescence enhancement with size of the polystyrene colloidal sphere indicated its dependence on the LSPRs of the substrates. The excitation wavelength of PCFOz and P3HT layers highly overlapped with LSPRs of PS300/Ag and PS400/Ag, respectively (see **Fig.S14a** and c). Accordingly, the maximum fluorescence enhancement for PCFOz and P3HT were 1.5-2.0 times as much as those on the disordered NSL samples as well as other Ag-capped 2-D colloidal crystals samples. The maximum absorption of MPS-PPV layer (460 nm) was between the LSPRs of PS300/Ag (410 nm) and PS400/Ag (560 nm). Excitation by 405 nm (see **Fig.S15**) could lead to significantly greater enhancement on PS300/Ag than the one excited by 460 nm. Further excitation wavelength scanning in

**Fig.7** demonstrated the correspondence between the excitation wavelength and the LSPR of the Ag-capped colloidal crystals is the key to the maximum fluorescence enhancement. Similar results were also observed for maximum fluorescence enhancement at  $\lambda_{\text{ex}}=560$  nm for P3HT (see **Fig.S16**).

Significantly higher enhancement ratio was observed from low quantum yield (QY) conjugated polymer of P3HT (QY~2%<sup>[18]</sup>), which was greater than 60 times (**Fig.6b**). For small fluorescent molecules of rhodamine B, fluorescein sodium and acriflavine, the enhancement ratios were generally smaller due to their high quantum yield. However, similar regularity for fluorescent enhancement could be observed: maximum fluorescence enhancements appeared on the substrates with LSPRs closest to their excitation wavelengths (see **Fig.S11-13**). For rhodamine B, the excitation wavelength highly overlapped with the LSPR of PS400/Ag (see **Fig.S14f**), and consequently its maximum fluorescence enhancement was about 1.36 times as much as those on PS300/Ag and PS600/Ag. For fluorescein sodium and acriflavine, whose maximum absorptions were between the LSPRs of PS300/Ag and PS400/Ag, the difference between their fluorescence enhancements on PS300/Ag and PS400/Ag became much smaller (less than 20%, see **Fig.S11** and **Fig.S13**).

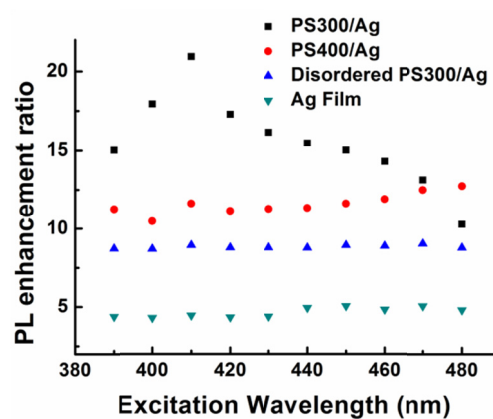


**Figure 7** Plots of the excitation wavelength for MPS-PPV layer versus the PL enhancement ratio on Ag film, PS300/Ag, PS400/Ag and disordered PS300/Ag.

### 3.3 Lifetime measurement

Recently, Geddes and co-workers reported that the underlying mechanism of MIFE could be underpinned by two complimentary effects: (1) an enhanced absorption and (2) an enhanced emission component.<sup>[19]</sup> In other words, MIFE mainly refers to the following two processes. The first is the enhancements by the localized surface plasmon resonances (LSPR) of the metallic nanostructure. Secondly, the metallic substrates could modify the fluorescence decay rates (both radiative and non-radiative), which could significantly change the fluorescence lifetime and quantum yield.

To prove that the observed fluorescence enhancement ratio changed with the colloidal crystal periods are mainly mediated by the correspondence between LSPR and the excitation wavelength, fluorescence lifetime measurements were

performed to analyze the effects of excitation enhancement ( $E_{ex}$ ) and emission enhancement ( $E_{em}$ ) based on a widely accepted semi-empirical model.<sup>[13c, 20]</sup>

It is well-known that when the observed emission of the fluorophore in the absence of any quenching interactions, the quantum yield of the fluorescence can be described by:<sup>[21]</sup>

$$Q_0 = \Gamma_0 / (\Gamma_0 + k_{nr}) \quad (3)$$

Where  $\Gamma_0$  is the fluorophore radiative rate and  $k_{nr}$  are the nonradiative rates. The observed lifetime,  $\tau_0$ , is subsequently described by:<sup>[21]</sup>

$$\tau_0 = 1 / (\Gamma_0 + k_{nr}) \quad (4)$$

In the presence of near-field metal substrates, it was suggested that the fluorophore should be described by a modified quantum yield and lifetime:<sup>[22]</sup>

$$Q_m = (\Gamma_0 + \Gamma_m) / (\Gamma_0 + \Gamma_m + \Gamma_{m,abs} + k_{nr}) \quad (5)$$

$$\tau_m = 1 / (\Gamma_0 + \Gamma_m + \Gamma_{m,abs} + k_{nr}) \quad (6)$$

where  $\Gamma_m$  is an additional radiative rate of the fluorophores near the plasmonic nanostructures and  $\Gamma_{m,abs}$  is the additional non-radiative decay rate.

We assumed that the fluorescence non-radiative decay rate was the same on quartz and metal substrates.  $\Gamma_{m,abs}$  was neglected as  $\Gamma_{m,abs}$  fell off rapidly with fluorophore-metal distance (over 10 nm in our substrates).<sup>[5, 22]</sup>

Utilizing the measured lifetime and Eqs.(3)-(6), we could calculate the emission enhancement ( $E_{em} = Q_m / Q_0$ ) of each samples. Hence the excitation enhancement ( $E_{ex}$ ) could be obtained by:<sup>[13c, 19, 20b]</sup>

$$E_{ex} = E_f / E_{em} \quad (7)$$

**Fig.8** shows the fluorescence lifetime spectra of PCFOz layer on PS200/Ag to PS 1000/Ag samples, as well as on a quartz surface as a control. The average lifetime of PCFOz layer on quartz was measured to be 787 ps. The lifetimes of PCFOz layer on PS200/Ag, PS300/Ag, PS400/Ag, PS600/Ag, and PS 1000/Ag samples were significantly reduced to 238, 183, 250, 280 and 327 ps, respectively.

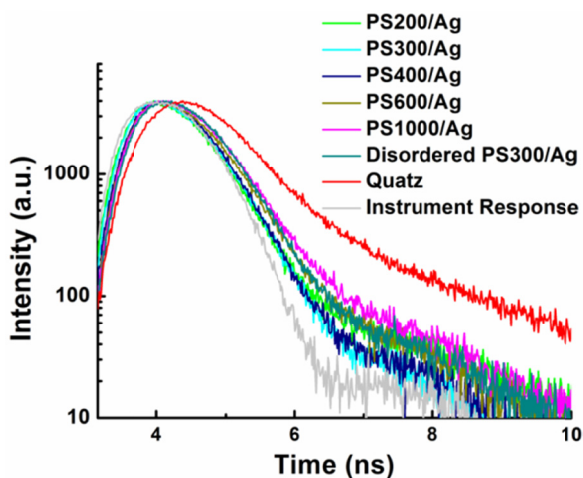


**Figure 8** PL lifetime measurement of PCFOz layer at 515 nm on quartz (~787 ps), PS200/Ag sample (~238 ps), PS300/Ag (~183 ps), PS400/Ag (~250 ps), PS600/Ag (~280 ps), PS1000/Ag (~327 ps), and disordered PS300/Ag, respectively.

The results of fitting to a multiexponential decay analysis with two decay times and the calculated quantum yields for PCFOz layer are presented in **Table 1**, with the quantum yield of PCFOz in free-space conditions ( $Q_0$ ) measured to be 0.35. The radiative decay rates and the resulting  $E_{em}$  of PCFOz were significantly increased on both the ordered and disordered Ag-capped 2-D colloidal crystals samples. As shown in Table 1,  $E_{ex}$  of PS300/Ag was 1.45 times to the one of disordered PS300/Ag sample while  $E_{em}$  of PS300/Ag was 1.14 times to the one of disordered PS300/Ag sample, indicating that the major contribution of LSPR was to increase the excitation.

**Table 1** The measured values of lifetime ( $\tau$ , ps), goodness of fit parameter ( $\chi_R^2$ ), quantum yield ratios ( $Q_m$ ) and the values of excitation enhancement and emission enhancement for each Ag-capped sample of PCFOz versus a quartz surface ( $Q_0=0.35$ ).

Sample	$\tau$	$\chi_R^2$	$Q_m$	$E_{em} = Q_m / Q_0$	$E_f$	$E_{ex}$
Quartz	787	1.32				
Ag-film	670	1.34	0.447	1.28	1.98	1.55
PS200/Ag	238	1.66	0.804	2.30	5.50	2.39
PS300/Ag	183	1.37	0.849	2.43	7.50	3.09
PS400/Ag	250	1.73	0.794	2.27	4.90	2.16
PS600/Ag	280	1.21	0.769	2.20	4.71	2.15
PS1000/Ag	327	1.17	0.730	2.09	4.40	2.11
Disordered PS300/Ag	303	1.44	0.750	2.14	4.56	2.13

The same tendency was observed for MPS-PPV and acriflavine as shown in **Table.S1** and **Table.S2**. In addition, all the calculated  $E_{ex}$  followed the exact trends with the  $E_f$  values. Such results are in good agreement with the correspondence between the excitation wavelength and the LSPR of the Ag-capped colloidal crystals, demonstrating that the maximum enhanced excitation and the hence  $E_f$  was caused by the maximum overlap between the excitation wavelength and LSPRs of the substrates.

Former works for small molecules fluorophores reported that the radiative decay rate was the largest on the substrates whose LSPR simultaneous overlapped with the excitation wavelength and emission wavelength of the fluorophores.<sup>[13c, 20b]</sup> However, the fluorescence emission of PCFOz in this work was efficiently overlapped with the LSPR wavelength of the PS400/Ag rather than PS300/Ag while the increase in the radiative decay rate and  $E_{em}$  for PCFOz were the largest on the PS300/Ag. For this inconsistency, we thought that the values of the lifetime measurements gave us an indication to the relative contribution of each process responsible for fluorescence enhancement but the precise values for  $E_{em}$  and  $E_{ex}$  were

difficult to determine because the model did not consider the coupling efficiency of the fluorescence emission to the far field.

## Conclusions

We have designed and fabricated a hybrid fluorescence enhancement system by vacuum coating silver films on 2-D colloid crystals with high robustness and reproducibility. Such Ag-capped 2-D colloid crystals could enhance fluorescence from conjugated polymers with low quantum yield (60 fold for P3HT) as well as dyes with high quantum yield (3.4 fold for rhodamine B). The work demonstrated that the maximum enhancement was attributed to the overlapping between LSPRs of the substrates and the excitation wavelength of the fluorophores rather than the emission wavelength. We expect that this approach could provide a guideline for fluorescence enhancement by SPR and find applications in fluorescence sensing and photovoltaic device.

## Acknowledgements

This work was supported by the National Natural Science Foundations of China (Grant no. 51173215 and 51233008).

## Notes and references

<sup>a</sup> Key Laboratory for Polymeric Composite and Functional Materials of Ministry of Education, School of Chemistry and Chemical Engineering, Sun Yat-sen University, Guangzhou, 510275, China. E-mail: cesxcd@mail.sysu.edu.cn; ceszmq@mail.sysu.edu.cn.

† Electronic Supplementary Information (ESI) available: SEM images and fluorescence spectra of PS400/Ag samples with different thickness of Ag cap, illustration and calculation results of the FDTD model, SEM images and extinction spectra for the disordered samples, fluorescence spectra of three small molecule fluorophores, absorption/emission spectra of the fluorophore layers with the corresponding LSPRs of the substrates, plots of the excitation wavelength for P3HT layer versus the PL enhancement ratio, the measured values of lifetime and the values of the excitation enhancement and emission enhancement for MPS-PPV and acriflavine. See DOI: 10.1039/b000000x/

‡ These authors contributed equally to this work.

- (a) H. I. Peng, C. M. Strohsahl, K. E. Leach, T. D. Krauss and B. L. Miller, *ACS Nano*, 2009, **3**, 2265; (b) Y. Wang, B. Liu, A. Mikhailovsky and G. C. Bazan, *Adv. Mater.*, 2010, **22**, 656; (c) Y. Cheng, T. Stakenborg, P. V. Dorpe, L. Lagae, M. Wang, H. Chen and G. Borghs, *Anal. Chem.*, 2011, **83**, 1307; (d) Y. Shan, J. J. Xu and H. Y. Chen, *Chem. Commun.*, 2009, 905; (e) K. Aslan, J. Huang, G. M. Wilson and C. D. Geddes, *J. Am. Chem. Soc.*, 2006, **128**, 4206; (f) H. Szmazinski, K. Ray and J. R. Lakowicz, *Anal. Biochem.*, 2009, **385**, 358; (g) C. R. Sabanayagam and J. R. Lakowicz, *Nucleic Acids Res.*, 2007, **35**, e13.
- (a) K. Aslan, J. R. Lakowicz and C. D. Geddes, *Curr. Opin. Chem. Biol.*, 2005, **9**, 538; (b) H. A. Atwater and A. Polman, *Nat. Mater.*, 2010, **9**, 205; (c) P. Kramper, M. Agio, C. M. Soukoulis, A. Birner, F. Müller, R. B. Wehrspohn, U. Gösele and V. Sandoghdar, *Phys. Rev. Lett.*, 2004, **92**, 113903.
- (a) J. Zhang, Y. Fu, D. Liang, K. Nowaczyk, R. Y. Zhao and J. R. Lakowicz, *Nano Lett.*, 2008, **8**, 1179; (b) A. Saha, S. K. Basiruddin, R. Sarkar, N. Pradhan and N. R. Jana, *J. Phys. Chem. C*, 2009, **113**, 18492; (c) J. Zhang, Y. Fu and J. R. Lakowicz, *J. Phys. Chem. C*, 2011, **115**, 7255.
- (a) K. H. Drexhage, *J. Lumin.*, 1970, **12**, 693; (b) G. W. Ford and W. H. Weber, *Surf. Sci.*, 1981, **109**, 451; (c) J. R. Lakowicz, C. D. Geddes, I. Gryczynski, J. Malicka, Z. Gryczynski, K. Aslan, J. Lukomska, E. Matveeva, J. Zhang, R. Badugu and J. Huang, *J. Fluoresc.*, 2004, **14**, 425; (d) K. Aslan, J. R. Lakowicz and C. D. Geddes, *Anal. Bioanal. Chem.*, 2005, **382**, 926; (e) K. Aslan, I. Gryczynski, J. Malicka, E. Matveeva, J. R. Lakowicz and C. D. Geddes, *Curr. Opin. Biotechnol.*, 2005, **16**, 55; (f) J. R. Lakowicz, *Anal. Biochem.*, 2005, **337**, 171.
- (a) J. I. Gersten, *Surf. Sci.*, 1985, **158**, 165; (b) J. R. Lakowicz, *Anal. Biochem.*, 2001, **298**, 1.
- (a) K. Li, M. I. Stockman and D. J. Bergman, *Phys. Rev. Lett.*, 2003, **91**, 227402; (b) S. H. Guo, S. J. Tsai, H. C. Kan, D. H. Tsai, M. R. Zachariah and R. J. Phaneuf, *Adv. Mater.*, 2008, **20**, 1424.
- L. J. Guo, *Adv. Mater.*, 2007, **19**, 495.
- (a) A. Kinkhabwala, Z. Yu, S. Fan, Y. Avlasevich, K. Müllen and W. E. Moerner, *Nat. Photonics*, 2009, **3**, 654; (b) K. Ray and J. R. Lakowicz, *J. Phys. Chem. C*, 2013, **117**, 15790.
- (a) R. Bardhan, N. K. Grady and N. J. Halas, *Small*, 2008, **4**, 1716; (b) B. Yang, N. Lu, D. Qi, R. Ma, Q. Wu, J. Hao, X. Liu, Y. Mu, N. Kehagias, C. M. S. Torres, F. Y. C. Boey, X. Chen and L. Chi, *Small*, 2010, **6**, 1038; (c) F. Xie, M. S. Baker and E. M. Goldys, *J. Phys. Chem. B*, 2006, **110**, 23085; (d) H. Szmazinski, R. Badugu, F. Mahdavi, S. Blair and J. R. Lakowicz, *J. Phys. Chem. C*, 2012, **116**, 21563; (e) Y. Chen, K. Munechika and D. S. Ginger, *Nano Lett.*, 2007, **7**, 690.
- (a) P. Anderson, M. Griffiths and V. R. Boveia, *Plasmonics*, 2006, **1**, 103; (b) C. D. Geddes, H. Cao, I. Gryczynski, Z. Gryczynski, J. Fang and J. R. Lakowicz, *J. Phys. Chem. A*, 2003, **107**, 3443; (c) K. H. Cho, S. I. Ahn, S. M. Lee, C. S. Choi and K. C. Choi, *Appl. Phys. Lett.*, 2010, **97**, 193306.
- (a) T. R. Jensen, M. D. Malinsky, C. L. Haynes and R. P. V. Duyne, *J. Phys. Chem. B*, 2000, **104**, 10549; (b) M. D. Malinsky, K. L. Kelly, G. C. Schatz and R. P. V. Duyne, *J. Phys. Chem. B*, 2001, **105**, 2343; (c) Y. Li, W. Cai and G. Duan, *Chem. Mater.*, 2008, **20**, 615; (d) D. K. Kim, S. M. Yoo, T. J. Park, H. Yoshikawa, E. Tamiya, J. Y. Park and S. Y. Lee, *Anal. Chem.*, 2011, **83**, 6215.
- (a) A. I. Maarroof, M. B. Cortie, N. Harris and L. Wiczorek, *Small*, 2008, **4**, 2292; (b) R. M. Cole, J. J. Baumberg, F. J. G. Abajo, S. Mahajan, M. Abdelsalam and P. N. Bartlett, *Nano Lett.*, 2007, **7**, 2094; (c) T. A. Kelf, Y. Sugawara, R. M. Cole, J. J. Baumberg, M. E. Abdelsalam, S. Cintra, S. Mahajan, A. E. Russell and P. N. Bartlett, *Phys. Rev. B*, 2006, **74**, 245415; (d) W. L. Barnes, A. Dereux and T. W. Ebbesen, *Nature*, 2003, **424**, 824.
- (a) B. Ding, C. Hrelescu, N. Arnold, G. Isic and T. A. Klar, *Nano Lett.*, 2013, **13**, 378; (b) P. P. Pompa, L. Martiradonna, A. Della Torre, F. D. Sala, L. Manna, M. D. Vittorio, F. Calabi, R. Cingolani and R. Rinaldi, *Nat. Immunol.*, 2006, **1**, 126; (c) F. Xie, J. S. Pang, A. Centeno, M. P. Ryan, D. J. Riley and N. M. Alford, *Nano Res.*,

- 2013, **6**, 496; (d) K. Sugawa, T. Tamura, H. Tahara, D. Yamaguchi, T. Akiyama, J. Otsuki, Y. Kusaka and N. Fukuda, *ACS Nano*, 2013, **7**, 9997.
- 14 (a) M. Li, S. K. Cushing, H. Liang, S. Suri, D. Ma and N. Wu, *Anal. Chem.*, 2013, **85**, 2072; (b) H. Im, K. C. Bantz, S. H. Lee, T. W. Johnson, C. L. Haynes and S. H. Oh, *Adv. Mater.*, 2013, **25**, 2678; (c) J. P. Camden, J. A. Dieringer, J. Zhao and R. P. V. Duyne, *Acc. Chem. Res.*, 2008, **41**, 1653; (d) M. Li, S. K. Cushing, J. Zhang, S. Suri, R. Evans, W. P. Petros, L. F. Gibson, D. Ma and Y. Liu, *ACS Nano*, 2013, **7**, 4967; (e) W. Huang, W. Qian and M. A. El-Sayed, *J. Phys. Chem. B.*, 2005, **109**, 18881.
- 15 Z. Huang, F. Sun, S. Liang, H. Wang, G. Shi, L. Tao and J. Tan, *Macromol. Chem. Phys.*, 2010, **211**, 1868.
- 16 F. Sun and J. C. Yu, *Angew. Chem. Int. Ed.*, 2007, **46**, 773.
- 17 W. Y. Wong, L. Liu, D. Cui, L. M. Leung, C. F. Kwong, T. H. Lee and H. F. Ng, *Macromolecules*, 2005, **38**, 4970.
- 18 S. Cook, A. Furube and R. Katoh, *Energy Environ. Sci.*, 2008, **1**, 294.
- 19 (a) Y. Zhang, A. Dragan and C. D. Geddes, *J. Phys. Chem. C*, 2009, **113**, 12095; (b) K. Aslan and C. D. Geddes, *Chem. Soc. Rev.*, 2009, **38**, 2556; (c) M. Weisenberg, Y. Zhang and C. D. Geddes, *Appl. Phys. Lett.*, 2010, **97**, 133103.
- 20 (a) A. I. Dragan and C. D. Geddes, *Appl. Phys. Lett.*, 2012, **100**, 093115; (b) F. Xie, M. S. Baker and E. M. Goldys, *Chem. Mater.*, 2008, **20**, 1788.
- 21 *Molecular Fluorescence: Principles and Applications*, B. Valeur, Wiley-VCH, Berlin, 2001.
- 22 *Principles of Fluorescence Spectroscopy*, J. R. Lakowicz, Springer Science and Business Media, LLC, New York, 2006.

A systematic study about the excitation wavelength-LSPR based fluorescence enhancement of conjugated polymers on Ag-capped two-dimensional colloidal crystals.

Keyword: Two-Dimensional Colloidal Crystals, Localized Surface Plasmon Resonances, Conjugated Polymers, Fluorescence Enhancement

By Wei Hong, Yu Zhang, Lin Gan, Xudong Chen\* and Mingqiu Zhang\*

Title: Control of Plasmonic Fluorescence Enhancement on Self-Assembled 2-D Colloidal Crystals

